



Alexandria University
Alexandria Engineering Journal

www.elsevier.com/locate/aej
www.sciencedirect.com



ORIGINAL ARTICLE

Effect of thermo-diffusion and parabolic motion on MHD second grade fluid flow with ramped wall temperature and ramped surface concentration

Hari R. Kataria^a, Harshad R. Patel^{b,*}

^a Department of Mathematics, Faculty of Science, The M. S. University of Baroda, Vadodara, India

^b Applied Science & Humanities Department, Sardar Vallabhbhai Patel Institute of Technology, Vasad, India

Received 29 June 2016; revised 20 October 2016; accepted 6 November 2016

KEYWORDS

MHD;
 Second grade fluid;
 Porous medium;
 Parabolic motion;
 Radiating;
 Surface concentration

Abstract In this paper, effects of parabolic motion, heat generation/absorption and thermo-diffusion on unsteady free convective MHD flow of radiating and chemically reactive second grade fluid near an infinite vertical plate through porous medium have been considered. It is assumed that the bounding plate has a ramped temperature with ramped surface concentration and isothermal temperature with ramped surface concentration. For finding the exact solution, we applied Laplace transform technique on the governing nondimensionalized equations. Analytic expression of Skin friction, Nusselt number and Sherwood number is derived and represented through tabular form. The effects of Magnetic parameter M , second grade fluid α , Heat generation/absorption H , thermal radiation parameter R , chemical reaction Kr and thermo-diffusion Sr on velocity, temperature and concentration profiles are discussed through several figures. We found that velocity, temperature and concentration profiles in case of ramped temperature with ramped surface concentrations are less than those of isothermal temperature with ramped surface concentrations. It is also seen that Magnetic field M , second grade fluid α and chemical reaction Kr have retarding effects on velocity profile, whereas thermo-diffusion parameter Sr and thermal radiation parameter R have reverse effects on it.

© 2016 Faculty of Engineering, Alexandria University. Production and hosting by Elsevier B.V. This is an open access article under the CC BY-NC-ND license (<http://creativecommons.org/licenses/by-nc-nd/4.0/>).

1. Introduction

Due to increasing significance, application of Non-Newtonian fluid is required in engineering. It is due to their numerous

applications in several areas, such as the plastic manufacture, performance of lubricants, food processing, or movement of biological fluids. Second grade fluids can model many fluids such as dilute polymer solutions, slurry flows, and industrial oils, and many flow problems with various geometries and different mechanical and thermal boundary conditions have been studied. Tan and Masuoka [1] examined the Stokes' first problem for a second grade fluid and Rashidi et al. [2] deal with unsteady squeezing flow of a second-grade fluid, whereas

* Corresponding author.

E-mail addresses: hkrmaths@yahoo.com (H.R. Kataria), harshadpatel2@gmail.com (H.R. Patel).

Peer review under responsibility of Faculty of Engineering, Alexandria University.

<http://dx.doi.org/10.1016/j.aej.2016.11.014>

1110-0168 © 2016 Faculty of Engineering, Alexandria University. Production and hosting by Elsevier B.V.

This is an open access article under the CC BY-NC-ND license (<http://creativecommons.org/licenses/by-nc-nd/4.0/>).

Nomenclature

| | |
|--------|---|
| u' | fluid velocity in x' direction |
| t' | time |
| T' | fluid temperature |
| B_0 | uniform magnetic field |
| k'_1 | permeability of porous medium |
| C' | concentration |
| k | thermal conductivity of the fluid |
| C_p | specific heat at constant pressure |
| q'_r | radiative heat flux |
| Q_0 | heat absorption/generation coefficient |
| D_M | mass diffusion coefficient |
| D_T | thermal diffusion coefficient |
| k'_2 | chemical reaction coefficient |
| u | dimensionless fluid velocity in x direction |
| t | dimensionless time |
| k_1 | permeability parameter |
| M | magnetic parameter |
| Gr | thermal Grashof number |
| Gm | mass Grashof number |

| | |
|----------|--------------------------------------|
| θ | dimensionless fluid temperature |
| C | dimensionless concentration |
| R | thermal radiation parameter |
| Pr | Prandtl number |
| H | heat generation/absorption parameter |
| Sc | Schmidt number |
| Sr | Soret number |
| Kr | Chemical reaction parameter |

Greek symbols

| | |
|-------------|--|
| ν | kinematic viscosity coefficient |
| α_1 | one of the material modules of second grade fluids |
| β'_T | volumetric coefficient of thermal expansion |
| β'_c | volumetric coefficient of concentration expansion |
| α | second grade parameter |
| ρ | fluid density |
| g | acceleration due to gravity |
| σ | electrical conductivity |
| \emptyset | porosity of the porous medium |

Hayat et al. [3] deal with unsteady stagnation point flow of second grade fluid with variable free stream.

MHD is a branch of fluid dynamics which studies the movement of an electrically conducting fluid in a magnetic field. Research works in the magneto hydrodynamics have been advanced significantly during the last few decades after the pioneer work of Hartmann [4] in liquid metal duct flows under external magnetic field. There are many applications for the parabolic motion such as solar cookers, solar concentrators and parabolic through solar collector. A parabolic concentrator type solar cooker has a wide range of applications such as baking, roasting and distillation. Solar concentrators have their applications in increasing the rate of evaporation of waste water, in food processing, for making drinking water from brackish and seawater. Murty et al. [5] deal with evaluation of thermal performance of heat exchanger unit for parabolic solar cooker and Raja et al. [6] deal with design and manufacturing of parabolic through solar collector system. Muthucumaraswamy and Geetha [7] discuss effects of parabolic motion on an isothermal vertical plate with constant mass flux. Akbar et al. [8] consider MHD stagnation point flow of Carreau fluid toward a permeable shrinking sheet. Sheikholeslami et al. [9–11] investigate Magnetic field effect on nanofluid flow, whereas Sheikholeslami and Ellahi [12] deal with three dimensional mesoscopic simulation of magnetic field effect on nanofluid. Sheikholeslami et al. [13] define the solution of forced convection heat transfer with variable magnetic field, and Sheikholeslami and Chamkha [14] study free convection heat transfer of a nanofluid in a semi-annulus enclosure with a sinusoidal wall, whereas specifically ferro-nanofluid is also discussed by Sheikholeslami et al. [15,16]. Kataria et al. [17] obtained the solution of effect of magnetic field on micropolar fluid between two vertical walls.

The radiations due to heat transfer effects on different flows are very important in space technology and high temperature processes. Thermal radiation parameter effects may play an important role in controlling heat transfer in polymer process-

ing industry. Many researchers like, Sheikholeslami et al. [18–19], and Kataria and Mittal [20] have discussed about effect of thermal radiation parameter on nanofluid flow. The basic law governing the flow of fluids through porous media is Darcy's Law. Importance of porous medium in MHD flow is presented by Nadeem et al. [21] and Kataria and Mittal [22]. On the other hand the research studies related to heat generating or heat absorbing fluid flow are of considerable importance in several physical problems viz. Abbasi et al. [23] deal with mixed convection flow of Maxwell nanofluid with heat generation, whereas Shehzad et al. [24] study three dimensional MHD Casson fluid flow with heat generation through porous medium and Fetecau et al. [25] deal with slip effects on radiative MHD flow over a moving plate with heat source. Some of the numerous important applications of heat and mass transfer flow with chemical reaction can be found in catalytic chemical reactors, food processing, polymer production, manufacture of ceramics and glassware, smelting, undergoing exothermic or endothermic chemical reaction. Kataria and Patel [26] deal with radiation and chemical reaction effect on MHD Casson fluid flow through porous medium. Such effects are significant when density differences exist in the flow regime. For example when species are introduced at a surface in fluid domain, with different (lower) densities than the surrounding fluid, Soret effects can be significant. The thermal diffusion (Soret) effect, for instance, has been utilized for isotope separation, and in mixture between gases with very light molecular weight (H_2 , He) and of medium molecular weight (N_2 , air). Sengupta and Ahmed [27] deal with MHD flow with thermal diffusion through embedded porous media, whereas Kataria and Patel [28] deal with soret and heat generation effect on MHD Casson fluid flow with radiation and reaction through embedded porous medium.

However, in all the investigations carried out by researchers considering ramped temperature profiles, it is to be noted that interval for ramped profile varies from material to material depending upon the specific heat capacity of the material.

Using Eq. (8) and dimensionless quantities, equations (1)–(4) become

$$\frac{\partial^2 u}{\partial y^2} + \alpha \frac{\partial^3 u}{\partial y^2 \partial t} - c \frac{\partial u}{\partial t} - bu + Gr\theta + GmC = 0 \quad (9)$$

$$\frac{\partial \theta}{\partial t} = \frac{1+R}{Pr} \frac{\partial^2 \theta}{\partial y^2} + \frac{H}{Pr} \theta \quad (10)$$

$$\frac{\partial C}{\partial t} = \frac{1}{Sc} \frac{\partial^2 C}{\partial y^2} + Sr \frac{\partial^2 \theta}{\partial y^2} - krC \quad (11)$$

With initial and boundary conditions

$$u = \theta = C = 0, \quad y \geq 0, \quad t \leq 0$$

$$u = t^2, \quad \theta = \begin{cases} t, & 0 < t \leq 1 \\ 1 & t > 1 \end{cases},$$

$$C = \begin{cases} t, & 0 < t \leq 1 \\ 1 & t > 1 \end{cases} \quad \text{at } y = 0, t > 0$$

$$u \rightarrow 0, \quad \theta \rightarrow 0, \quad C \rightarrow 0 \quad \text{at } y \rightarrow \infty, \quad t > 0 \quad (12)$$

where

$$\alpha = \frac{\alpha_1}{\rho \nu t_0}, \quad Gr = \frac{g \beta'_T (T'_w - T'_\infty)}{U_0 t_0}, \quad M^2 = \frac{\sigma B_0^2}{\rho U_0 t_0},$$

$$\frac{1}{k_1} = \frac{U_0 \nu t_0^2 \varnothing}{k'_1}, \quad Gm = \frac{g \beta'_C (C'_w - C'_\infty)}{U_0 t_0}, \quad Pr = \frac{\rho \nu C_p}{k},$$

$$R = \frac{16 \sigma^* T_\infty^3}{3 k k^*}, \quad H = \frac{Q_0 \nu t_0}{k}, \quad Sc = \frac{\nu}{D_M}, \quad Sr = \frac{D_T (T'_w - T'_\infty)}{\nu (C'_w - C'_\infty)},$$

$$Kr = t_0 k'_2, \quad c = 1 + \frac{\alpha}{k_1}, \quad b = M^2 + \frac{1}{k_1}$$

$$\text{For Simplicity, } t_0 = \left(\frac{\nu}{U_0^2} \right)^{1/5}$$

Exact solution for fluid velocity; Temperature and Concentration are obtained for equations (9)–(11) with initial and boundary condition (12) using the Laplace transform technique.

3. Solution of the problem for ramped wall temperature and ramped surface concentration

$$\theta(y, t) = f_6(y, t, L, a_1) - f_6(y, t-1, L, a_1)H(t-1) \quad (13)$$

$$C(y, t) = [f_6(y, t, Sc, ScKr) + f_8(y, t, Sc, ScKr) - f_8(y, t, L, a_1)] \\ - [f_6(y, t-1, Sc, ScKr) + f_8(y, t-1, Sc, ScKr) \\ - f_8(y, t-1, L, a_1)]H(t-1) \quad (14)$$

$$u(y, t) = [g_1(y, t) + g_2(f_3(t), f_9(y, t, Sc, ScKr)) \\ + g_2(f_4(t), f_9(y, t, L, a_1))] \\ - [g_1(y, t-1) + g_2(f_3(t-1), f_9(y, t-1, Sc, ScKr)) \\ + g_2(f_4(t-1), f_9(y, t-1, L, a_1))]H(t-1) \quad (15)$$

4. Solution of the problem for isothermal temperature and ramped surface concentration

In order to understand effects of ramped temperature of the plate on the fluid flow, we must compare our results with

isothermal temperature. In this case, the initial and boundary conditions are the same excluding Eq. (12) that becomes $\theta = 1$ at $y = 0, \quad t \geq 0$.

$$\theta(y, t) = f_5(y, t, L, a_1) \quad (16)$$

$$C(y, t) = [f_6(y, t, Sc, ScKr) - f_6(y, t-1, Sc, ScKr)H(t-1) \\ + f_{12}(y, t, Sc, ScKr) - f_{12}(y, t, L, a_1)] \quad (17)$$

$$u(y, t) = g_1(y, t) + g_2(f_{10}(t), f_9(y, t, L, a_1)) \\ + g_3(f_{11}(t, a_9, a_{10}, a_{11}), f_9(y, t, Sc, ScKr)) \\ - g_3(f_{11}(t-1, a_9, a_{10}, a_{11}), f_9(y, t \\ - 1, Sc, ScKr)) \\ + g_3(f_{11}(t, a_{30}, a_{31}, a_{32}), f_9(y, t, Sc, ScKr)) \quad (18)$$

where

$$f_1(t) = 2t \quad (19)$$

$$f_2(y, t) = \frac{c}{\alpha} e^{-t/\alpha} \int_0^\infty \operatorname{erfc}\left(\frac{y}{2\sqrt{z}}\right) e^{-cz/\alpha} I_0\left(\frac{2}{\alpha} \sqrt{(c-\alpha b)zt}\right) dz \\ + \frac{b}{\alpha} \int_0^\infty \int_0^t \operatorname{erfc}\left(\frac{y}{2\sqrt{z}}\right) e^{-\frac{cz+\alpha s}{\alpha}} I_0\left(\frac{2}{\alpha} \sqrt{(c-\alpha b)zs}\right) ds dz \quad (20)$$

$$f_3(t) = a_{23} + a_{24}e^{b_9 t} + a_{25}e^{b_{10} t} + a_{13}e^{-a_4 t} \quad (21)$$

$$f_4(t) = a_{26} + a_{27}e^{b_4 t} + a_{28}e^{b_5 t} - a_{20}e^{-a_4 t} \quad (22)$$

$$f_5(y, t, a, b) = \frac{1}{2} \left[e^{-y\sqrt{b}} \operatorname{erfc}\left(\frac{y}{2\sqrt{t}} - \sqrt{bt}\right) + e^{y\sqrt{b}} \operatorname{erfc}\left(\frac{y}{2\sqrt{t}} + \sqrt{bt}\right) \right] \quad (23)$$

$$f_6(y, t, a, b) = \frac{1}{2} \left[\left(t - \frac{y}{2\sqrt{b}} \right) e^{-y\sqrt{b}} \operatorname{erfc}\left(\frac{y}{2\sqrt{t}} - \sqrt{bt}\right) \right. \\ \left. + \left(t + \frac{y}{2\sqrt{b}} \right) e^{y\sqrt{b}} \operatorname{erfc}\left(\frac{y}{2\sqrt{t}} + \sqrt{bt}\right) \right] \quad (24)$$

$$f_7(y, t, a, b) = \frac{e^{-at}}{2} \left[e^{-y\sqrt{\frac{1}{a}(b-a)}} \operatorname{erfc}\left(\frac{y}{2\sqrt{t}} - \sqrt{(b-a)t}\right) \right. \\ \left. + e^{y\sqrt{\frac{1}{a}(b-a)}} \operatorname{erfc}\left(\frac{y}{2\sqrt{t}} + \sqrt{(b-a)t}\right) \right] \quad (25)$$

$$f_8(y, t, a, b) = a_8 f_5(y, t, a, b) + a_6 f_6(y, t, a, b) + a_7 f_7(y, t, a, b) \quad (26)$$

$$f_9(y, t, a, b) = f_2(y, t) - f_5(y, t, a, b) \quad (27)$$

$$f_{10}(t) = -a_{33} + a_{36}e^{b_4 t} + a_{37}e^{b_5 t} \quad (28)$$

$$f_{11}(t, p, q, r) = p + qe^{b_9 t} + re^{b_{10} t} \quad (29)$$

$$f_{12}(y, t, a, b) = a_6 f_5(y, t, a, b) + a_{38} f_7(y, t, a, b) \quad (30)$$

$$g_1(y, t) = \int_0^t f_2(y, u) f_1(t-u) du \quad (31)$$

$$g_2(f_i(t), f_j(y, t, a, b)) = \int_0^t f_j(y, u, a, b) f_i(t-u) du \quad (32)$$

$$g_3(f_i(t, p, q, r), f_j(y, t, a, b)) = \int_0^t f_j(y, u, a, b) f_i(t-u, p, q, r) du \quad (33)$$

5. Skin friction, Nusselt number and Sherwood number

Expressions of Skin friction τ , Nusselt number Nu and Sherwood number Sh are calculated from Eqs. (13)–(18) using the relation

$$\tau_w(t) = -\tau(y, t) \text{ at } y = 0, \tau(y, t) = \left(1 + \alpha \frac{\partial}{\partial t}\right) \frac{\partial u}{\partial y} \Big|_{y=0},$$

$$Nu = -\left(\frac{\partial \theta}{\partial y}\right)_{y=0} \text{ and } Sh = -\left(\frac{\partial C}{\partial y}\right)_{y=0} \quad (34)$$

5.1. For ramped wall temperature and ramped surface concentration

$$\frac{\partial u}{\partial y} \Big|_{y=0} = [I_8(t) + I_9(t, Sc, ScKr) + I_9(t, L, a_1)] - [I_8(t-1) + I_9(t-1, Sc, ScKr) + I_9(t-1, L, a_1)]H(t-1) \quad (35)$$

$$Nu = -[I_3(t, L, a_1) - I_3(t-1, L, a_1)H(t-1)] \quad (36)$$

$$Sh = -[I_3(t, Sc, ScKr) + I_5(t, Sc, ScKr) - I_5(t, L, a_1)] + [I_3(t-1, Sc, ScKr) + I_5(t-1, Sc, ScKr) - I_5(t-1, L, a_1)]H(t-1) \quad (37)$$

5.2. For isothermal temperature and ramped surface concentration

$$\frac{\partial u}{\partial y} \Big|_{y=0} = [I_8(t) + I_9(t, L, a_1) + I_{10}(t, a_9, a_{10}, a_{11}, Sc, ScKr) - I_{10}(t-1, a_9, a_{10}, a_{11}, Sc, ScKr) + I_{10}(t, a_{30}, a_{31}, a_{32}, Sc, ScKr)] \quad (38)$$

$$Nu = -[I_2(t, L, a_1)] \quad (39)$$

$$Sh = -[I_3(t, Sc, ScKr) - I_6(t-1, Sc, ScKr)H(t-1) + I_{12}(t, Sc, ScKr) - I_{12}(t, L, a_1)] \quad (40)$$

where

$$I_1(t) = \frac{df_2(y, t)}{dy} \Big|_{y=0} = \frac{c}{\alpha\sqrt{\pi}} e^{-t/\alpha} \int_0^\infty \frac{e^{-cz/\alpha}}{\sqrt{z}} I_0\left(\frac{2}{\alpha} \sqrt{(c-\alpha b)zt}\right) dz - \frac{b}{\alpha\sqrt{\pi}} \int_0^\infty \int_0^t \frac{e^{-\frac{cz+\alpha}{s}}}{\sqrt{z}} I_0\left(\frac{2}{\alpha} \sqrt{(c-\alpha b)zs}\right) ds dz \quad (41)$$

$$I_2(t, a, b) = \frac{df_3(y, t)}{dy} \Big|_{y=0} = -\sqrt{b} \operatorname{berf}\left(\sqrt{\frac{b}{a}} t\right) + \sqrt{\frac{a}{\pi t}} e^{-\frac{b}{a}t} \quad (42)$$

$$I_3(t, a, b) = \frac{df_6(y, t, a, b)}{dy} \Big|_{y=0} = -\sqrt{\frac{a^2}{4b}} \operatorname{erf}\left(\sqrt{\frac{b}{a}} t\right) - t\sqrt{b} \operatorname{berf}\left(\sqrt{\frac{b}{a}} t\right) + \sqrt{\frac{ta}{\pi}} e^{-\frac{b}{a}t} \quad (43)$$

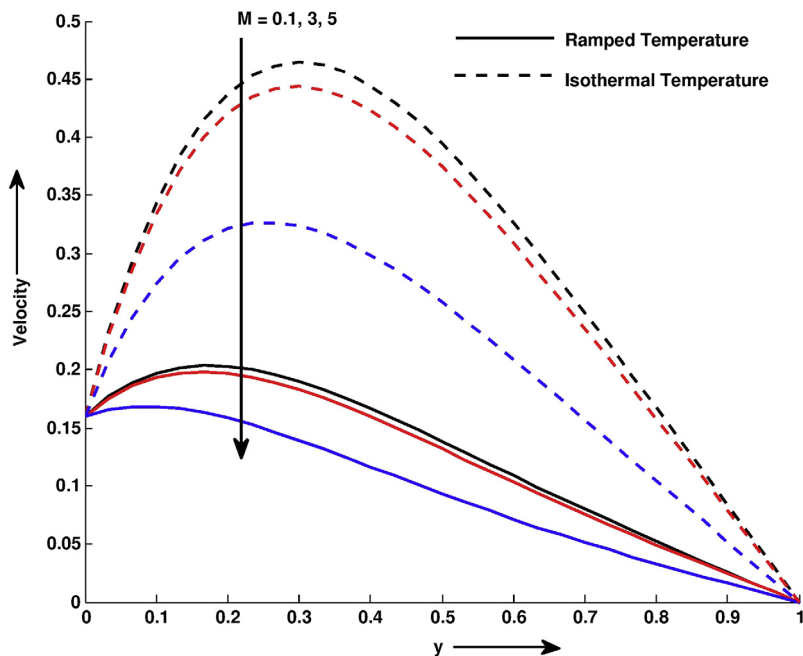


Figure 2 Velocity profile u for different values of y and M at $k = 0.8, Pr = 7, \alpha = 0.5, Sc = 0.66, Gm = 5, Gr = 10, Sr = 3, Kr = 2, H = 3, t = 0.4$ and $R = 5$.

$$I_4(t, a, b) = \left. \frac{df_7(y, t, a, b)}{dy} \right|_{y=0} = -e^{-a_4 t} \sqrt{(b - a a_4)} \operatorname{erf} \left(\sqrt{\left(\frac{b}{a} - a_4 \right) t} \right) + \sqrt{\frac{a}{\pi t}} e^{-\frac{b}{a} t} \quad (44)$$

$$I_6(t, a, b) = \left. \frac{df_9(y, t, a, b)}{dy} \right|_{y=0} = I_1(t) - I_2(t, a, b) \quad (46)$$

$$I_7(t, a, b) = \left. \frac{df_{10}(y, t, a, b)}{dy} \right|_{y=0} = a_6 I_2(t, a, b) + a_{38} I_4(t, a, b) \quad (47)$$

$$I_5(t, a, b) = \left. \frac{df_8(y, t, a, b)}{dy} \right|_{y=0} = a_8 I_2(t, a, b) + a_6 I_3(t, a, b) + a_7 I_4(t, a, b) \quad (45)$$

$$I_8(t) = \left. \frac{dg_1(y, t)}{dy} \right|_{y=0} \int_0^t I_1(u) f_1(t - u) du \quad (48)$$

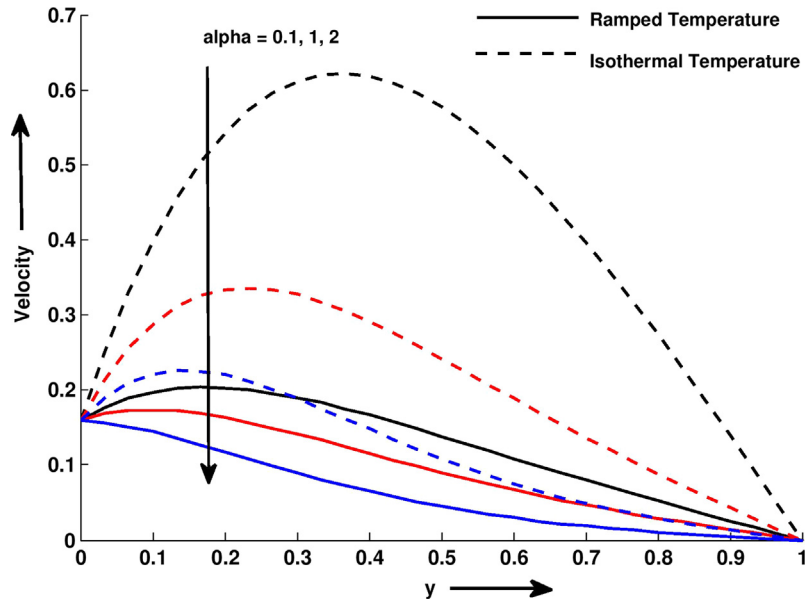


Figure 3 Velocity profile u for different values of y and α at $k = 0.8, Pr = 7, M = 0.5, Sc = 0.66, Gm = 5, Gr = 10, Sr = 3, Kr = 2, H = 3, t = 0.4$ and $R = 5$.

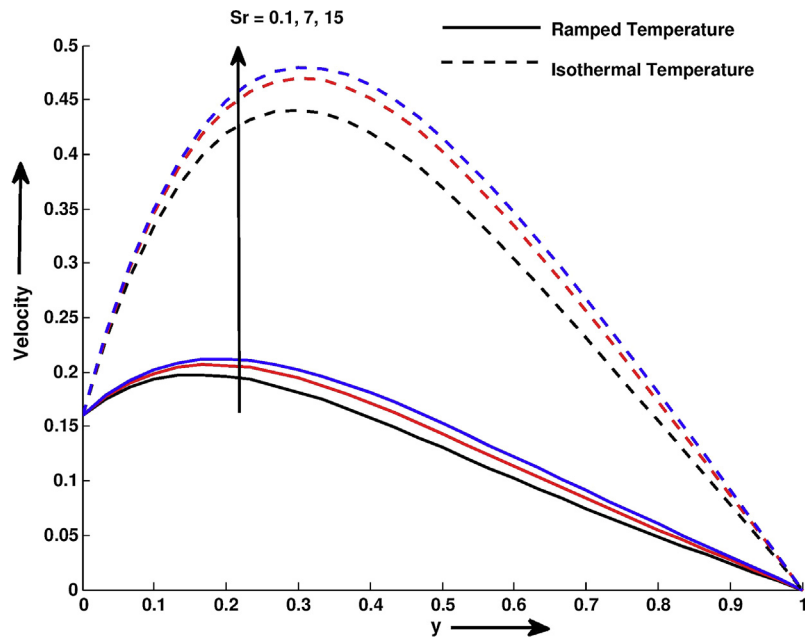


Figure 4 Velocity profile u for different values of y and Sr at $k = 0.8, Pr = 7, \alpha = 0.5, Sc = 0.66, Gm = 5, Gr = 10, M = 0.5, Kr = 2, H = 3, t = 0.4$ and $R = 5$.

$$I_9(t, a, b) = \frac{dg_2((f_i(t), f_j(y, t, a, b)))}{dy}$$

$$= \int_0^t I_j(u, a, b) f_i(t - u) du \quad (49)$$

$$I_{10}(t, p, q, r, a, b) = \frac{dg_2(f_i(t, p, q, r), f_j(y, t, a, b))}{dy}$$

$$= \int_0^t I_j(y, u, a, b) f_i(t - u, p, q, r) du \quad (50)$$

6. Numerical result and discussion

We have presented the fluid velocity, temperature and concentration for several values of Second grade parameter α , Magnetic field M , thermo-diffusion parameter Sr , thermal radiation parameter R , chemical reaction parameter Kr and Heat generation/absorption H described in Figs. 2–11.

From Figs. 2–11, it is depicted that velocity, temperature and concentration profiles are less in case of ramped tempera-

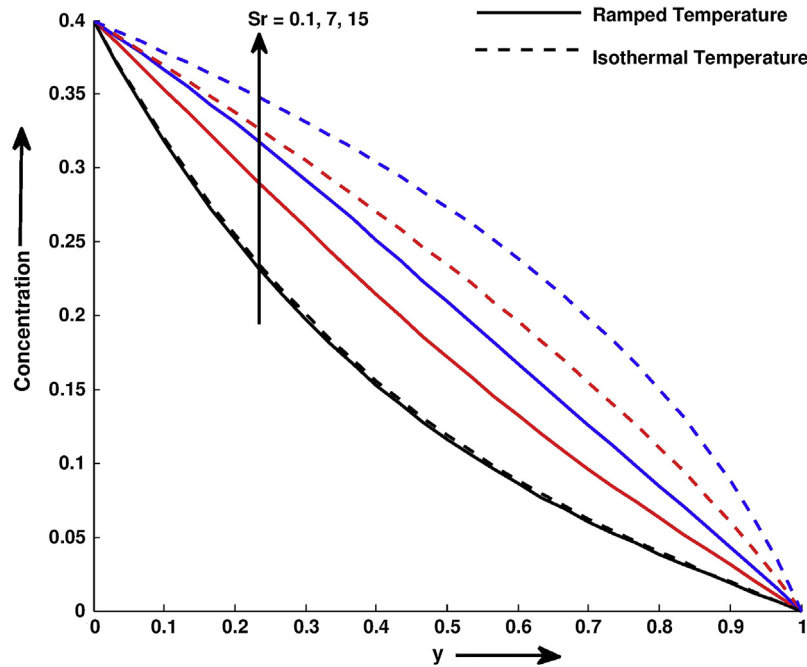


Figure 5 Concentration profile C for different values of y and Sr at $Pr = 7, Sc = 0.66, Kr = 2, H = 3, t = 0.4$ and $R = 5$.

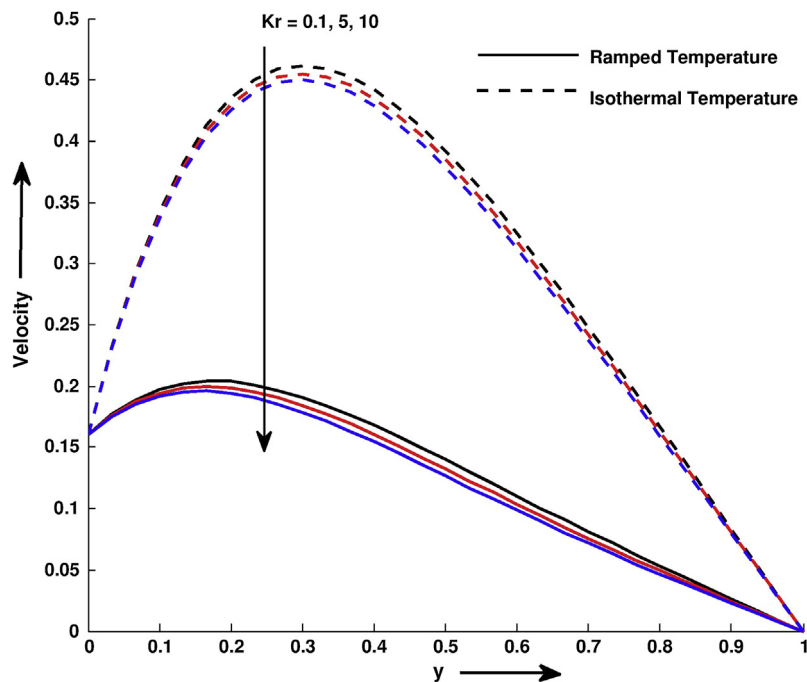


Figure 6 Velocity profile u for different values of y and Kr at $k = 0.8, Pr = 7, \alpha = 0.5, Sc = 0.66, Gm = 5, Gr = 10, Sr = 3, M = 0.5, H = 3, t = 0.4$ and $R = 5$.

ture with ramped surface concentration than those of isothermal temperature with ramped concentration.

Fig. 2 shows that Magnetic field has retarding effect on Velocity profile for both thermal conditions. We know that the presence of magnetic parameter generates electric field in the flow. This implies that magnetic field has retarding effect

for both ramped temperature with ramped surface concentration and isothermal temperature with Ramped surface concentrations. This is due to point that the application of a magnetic field to fluid gives increase to a resistive-type force (Lorentz force) on the fluid in the boundary layer, which slows down the motion of the fluid. Fig. 3 shows effects of second grade

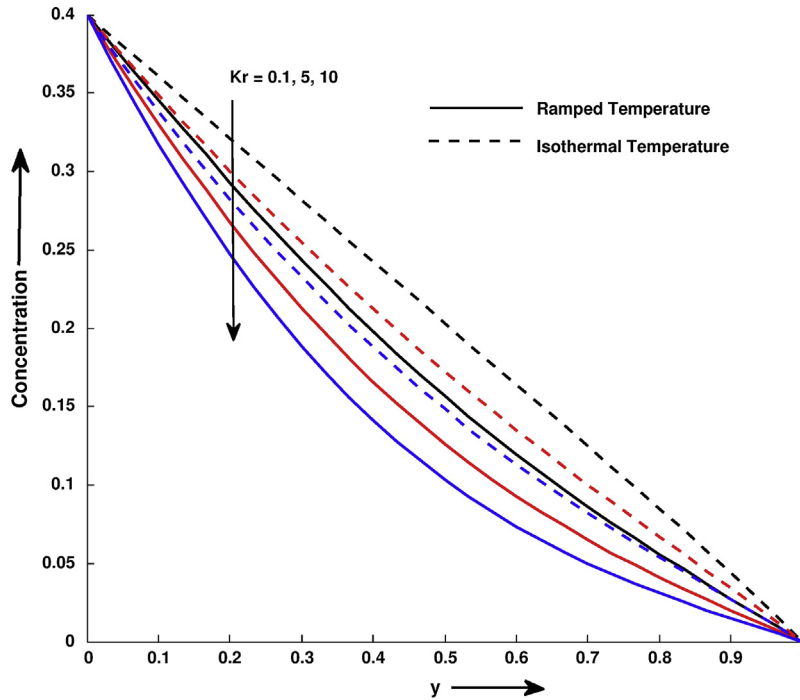


Figure 7 Concentration profile C for different values of y and Kr at $Pr = 7, Sc = 0.66, Sr = 3, H = 3, t = 0.4$ and $R = 5$.

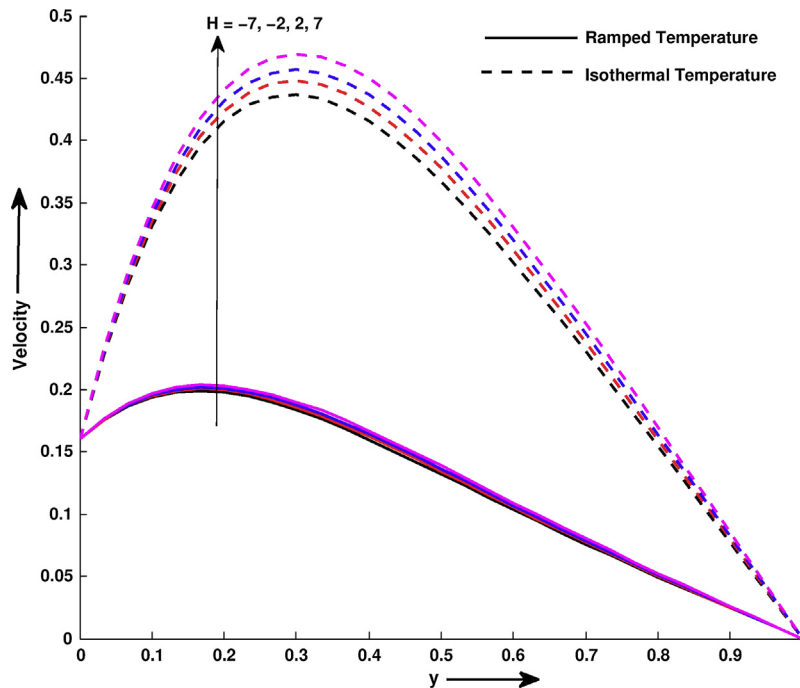


Figure 8 Velocity profile u for different values of y and H at $k = 0.8, Pr = 7, \alpha = 0.5, Sc = 0.66, Gm = 5, Gr = 10, Sr = 3, Kr = 2, M = 0.5, t = 0.4$ and $R = 5$.

parameter α on velocity for both thermal plates. It is seen that velocity decreases throughout the flow field with increase in second grade parameter α . It is also noticed that, the thickness of the boundary layer increases if the second grade parameter decreases. Figs. 4 and 5 exhibit the effects of thermo-diffusion Sr on velocity and concentration profile. For both thermal cases, velocity and concentration profile increases with increase in Sr . Physically, increase in values of Sr produces a

raise in the mass buoyancy force which results in an increase in the value of velocity profile as well as concentration profile, and thus thermo-diffusion tends to accelerate fluid flow in velocity flow directions throughout the boundary layer region. Chemical reaction has a retarding influence on fluid flow velocity and concentration profile for both thermal cases as shown in Figs. 6 and 7. This shows that the destructive reaction $Kr > 0$ leads to fall in the concentration field which in turn

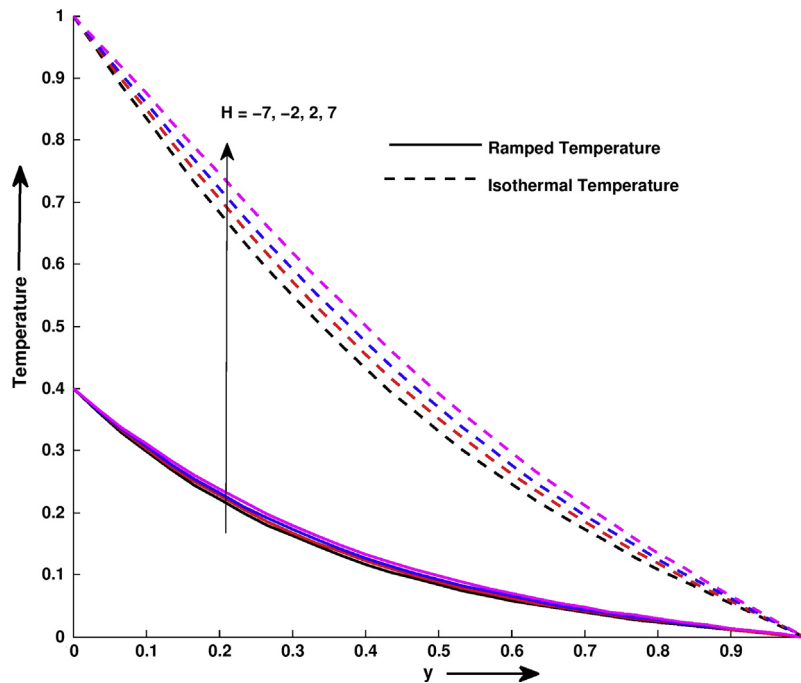


Figure 9 Temperature profile θ for different values of y and H at $Pr = 7, t = 0.4$ and $R = 5$.

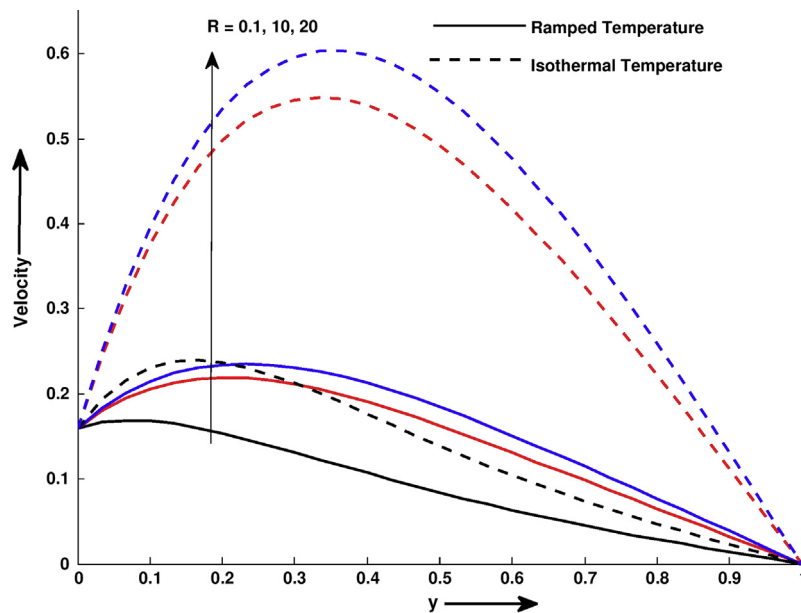


Figure 10 Velocity profile u for different values of y and R at $k = 0.8, Pr = 7, \alpha = 0.5, Sc = 0.66, Gm = 5, Gr = 10, Sr = 3, Kr = 2, H = 3, t = 0.4$ and $M = 0.5$.

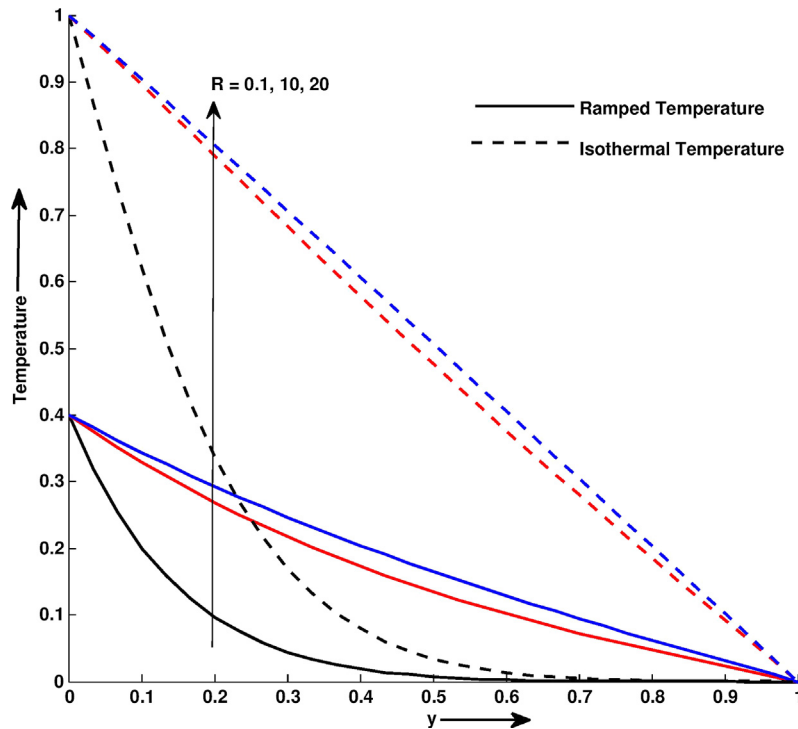


Figure 11 Temperature profile θ for different values of y and R at $Pr = 7$, $t = 0.4$ and $H = 3$.

weakens the buoyancy effects due to concentration gradients. Consequently, the flow field is retarded. This occurrence has a superior agreement with the physical realities. These results are in good agreement with the outcomes of work of Kataria and Patel [28]. Figs. 8 and 9 show the effects of heat generation/absorption H on velocity and temperature profiles. The positive sign indicates the heat generation (heat source) whereas negative means heat absorption (heat sink). Heat source physically implies generation of heat, which increases the temperature in the flow field. Therefore, as heat source parameter increased, the temperature increases steeply. The influence of heat source parameter $Q_0 > 0$ on velocity and temperature profiles is very much significantly related to the heat sink parameter $Q_0 < 0$. These results are clearly supported from the physical point of view because heat source implies generation of heat from the surface of the region,

and half of the porous is also increased which rises the temperature in the flow field. Therefore, velocity and temperature profiles increase with increase in H for both thermal plates. Thermal radiation parameter has a retarding influence on fluid flow velocity and temperature profile for both thermal cases as shown in Fig. 10 and 11. It is noticed that thermal radiation parameter reduces thermal buoyancy force, minimizing the thickness of the thermal boundary layer. Therefore velocity and temperature profiles increase with radiation parameter R . Physically, when the amount of heat generated through thermal radiation parameter increases, the bond holding the

Table 1 Nusselt number variation.

| H | R | Pr | t | Nusselt number Nu for ramped temperature | Nusselt number Nu for isothermal temperature |
|-----|-----|------|-----|--|--|
| -1 | 5 | 7 | 0.4 | 0.7854 | 1.0181 |
| -2 | 5 | 7 | 0.4 | 0.7999 | 1.0716 |
| -3 | 5 | 7 | 0.4 | 0.8141 | 1.1242 |
| -1 | 6 | 7 | 0.4 | 0.7272 | 0.9426 |
| -1 | 7 | 7 | 0.4 | 0.6802 | 0.8817 |
| -1 | 5 | 10 | 0.4 | 0.9336 | 1.1974 |
| -1 | 5 | 15 | 0.4 | 1.1384 | 1.4479 |
| -1 | 5 | 7 | 0.5 | 0.8822 | 0.9226 |
| -1 | 5 | 7 | 0.6 | 0.9708 | 0.8532 |

Table 2 Sherwood Number variation.

| Sr | Sc | Pr | Kr | H | R | t | Sherwood number Sh for ramped temperature | Sherwood number Sh for isothermal temperature |
|------|------|------|------|-----|-----|-----|---|---|
| 2 | 0.66 | 7 | 2 | -1 | 5 | 0.4 | 0.1852 | 0.1399 |
| 3 | 0.66 | 7 | 2 | -1 | 5 | 0.4 | -0.0838 | -0.1518 |
| 4 | 0.66 | 7 | 2 | -1 | 5 | 0.4 | -0.3528 | -0.4435 |
| 2 | 0.8 | 7 | 2 | -1 | 5 | 0.4 | 0.1744 | 0.1291 |
| 2 | 1.0 | 7 | 2 | -1 | 5 | 0.4 | 0.1569 | 0.1131 |
| 2 | 0.66 | 10 | 2 | -1 | 5 | 0.4 | 0.0308 | -0.0273 |
| 2 | 0.66 | 15 | 2 | -1 | 5 | 0.4 | -0.1935 | -0.2775 |
| 2 | 0.66 | 7 | 3 | -1 | 5 | 0.4 | 0.2737 | 0.2755 |
| 2 | 0.66 | 7 | 4 | -1 | 5 | 0.4 | 0.3555 | 0.3937 |
| 2 | 0.66 | 7 | 2 | -2 | 5 | 0.4 | 0.1702 | 0.0854 |
| 2 | 0.66 | 7 | 2 | -3 | 5 | 0.4 | 0.1553 | 0.0317 |
| 2 | 0.66 | 7 | 2 | -1 | 6 | 0.4 | 0.2437 | 0.2076 |
| 2 | 0.66 | 7 | 2 | -1 | 7 | 0.4 | 0.2897 | 0.2605 |
| 2 | 0.66 | 7 | 2 | -1 | 5 | 0.5 | 0.2534 | 0.3450 |
| 2 | 0.66 | 7 | 2 | -1 | 5 | 0.6 | 0.3261 | 0.5250 |

Table 3 Comparison of Nusselt number with Ref. [31] at $Pr = 0.71$.

| R | $\varnothing = -H/Pr$ | t | Nusselt number Nu for ramped temp. Ref [31] | Nusselt number Nu for ramped temp. | Nusselt number Nu for isothermal temp. Ref [31] | Nusselt number Nu for isothermal temp. |
|-----|-----------------------|-----|---|--------------------------------------|---|--|
| 2 | 3 | 0.3 | 0.38368 | 0.3837 | 0.89492 | 0.8949 |
| 2 | 3 | 0.5 | 0.55828 | 0.5583 | 0.85907 | 0.8591 |
| 2 | 3 | 0.7 | 0.72887 | 0.7289 | 0.84872 | 0.8487 |
| 2 | 1 | 0.5 | 0.44983 | 0.4498 | 0.56755 | 0.5675 |
| 2 | 3 | 0.5 | 0.55828 | 0.5583 | 0.85907 | 0.8591 |
| 2 | 5 | 0.5 | 0.65207 | 0.6521 | 1.09210 | 1.0921 |
| 2 | 3 | 0.5 | 0.55828 | 0.5583 | 0.85907 | 0.8591 |
| 4 | 3 | 0.5 | 0.43244 | 0.4324 | 0.66543 | 0.6654 |
| 6 | 3 | 0.5 | 0.36548 | 0.3655 | 0.56239 | 0.5624 |

Table 4 Comparison of Sherwood number with Ref. [32] at $Sr = 0$.

| t | Kr | Sc | Sherwood number Sh for ramped temp. Ref [32] | Sherwood number Nu for ramped temp. | Sherwood number Sh for isothermal temp. Ref [32] | Sherwood number Nu for isothermal temp. |
|-----|------|------|--|---------------------------------------|--|---|
| 0.3 | 0.2 | 0.22 | 0.295649 | 0.2956 | 0.525702 | 0.5257 |
| 0.5 | 0.2 | 0.22 | 0.386593 | 0.3866 | 0.428415 | 0.4284 |
| 0.7 | 0.2 | 0.22 | 0.463189 | 0.4632 | 0.379505 | 0.3796 |
| 0.3 | 2.0 | 0.22 | 0.344659 | 0.3447 | 0.839945 | 0.8399 |
| 0.5 | 2.0 | 0.22 | 0.488076 | 0.4881 | 0.785973 | 0.7860 |
| 0.7 | 2.0 | 0.22 | 0.625355 | 0.6254 | 0.757863 | 0.7579 |
| 0.3 | 5.0 | 0.22 | 0.416933 | 0.4169 | 1.1897 | 1.1897 |
| 0.5 | 5.0 | 0.22 | 0.628694 | 0.6287 | 1.12945 | 1.1294 |
| 0.7 | 5.0 | 0.22 | 0.838894 | 0.8389 | 1.09522 | 1.0952 |

components of the fluid particles is easily broken and the fluid velocity will increase. Thus, it is pointed out that the radiation should be minimized to have the cooling process at a faster rate.

The variation of the Nusselt Number and Sherwood Number is shown in Tables (1–2) for various values of the governing parameters. It is observed from Tables 1 that, for both thermal cases, Thermal radiation parameter tends to reduce the Nusselt number, whereas magnitude of heat absorption parameter H and Prandtl number Pr has reverse effect on it. It is also seen that, for ramped wall temperature, time variable t tends to improve rate of heat transfer, whereas for isothermal plates, time variable t have reverse effect on it. Table 2 illustrates the effects of Pr , Sc , Sr , R , Kr , H and t on rate of mass transfer Sh . For both thermal conditions, Sherwood number increases with increase in thermal radiation parameter R , chemical reaction Kr and time variable t whereas it decreases with an increase in Soret number Sr , Schmidt number Sc , Prandtl number Pr and magnitude of heat generation/absorption H . Table 3 validates our results in terms of Nusselt number as it shows strong agreement with Seth et al. [31] whereas Table 4 strengthens values of Sherwood number by comparing with those of Seth et al. [32].

8. Conclusion

The purpose of this study was to obtain exact solutions for effect of Parabolic motion on unsteady natural convective second grade fluid with thermal radiation parameter, chemical

reaction, soret and heat generation effects past over an infinite vertical plate through porous medium in the presence of a transverse uniform magnetic field. The effects of the pertinent parameters on velocity, concentration and temperature profiles are presented graphically. The most important concluding remarks can be summarized as follows:

- It is observed that velocity, temperature and concentration profiles in case of ramped temperature with ramped surface concentrations are less than those of isothermal temperature with ramped surface concentrations.
- Effect of all parameters is similar in ramped temperature with ramped surface concentration and isothermal temperature with constant surface concentration.
- Magnetic field M , second grade parameter α and chemical reaction parameter Kr delay velocity of the fluid flow throughout the boundary layer.
- Thermo-diffusion Sr , thermal radiation parameter R and heat generation tend to improve velocity.
- Temperature profile increases tendency with heat generation parameter H and thermal radiation parameter.
- Chemical reaction Kr tends to reduce concentration profile, whereas thermo-diffusion Sr has reverse effect on it.
- Thermal radiation parameter tends to reduce rate of heat transfer, whereas heat generation parameter H and Prandtl number Pr have reverse effect on it.
- Thermo-diffusion Sr tends to decrease rate of mass transfer, whereas chemical reaction and time variable t have reverse effects on it.

Appendix A

$$\begin{aligned}
c &= 1 + \frac{\alpha}{k_1} \\
a_2 &= a_1 - Kr.Sc \\
a_5 &= \frac{Sr.Sc}{a_3} \\
a_8 &= \frac{a_5(a_1+L)}{1+a_4} - a_6 - \frac{a_7}{1+a_4} \\
a_{11} &= \frac{Gm}{b_{10}(b_{10}-b_9)} \\
a_{14} &= \frac{Gmas(a_1+b_9L)}{(b_9)(b_9+a_4)(b_9-b_{10})} \\
a_{17} &= \frac{Gr}{(b_4)(b_4-b_5)} \\
a_{20} &= \frac{Gmas(a_1-a_4L)}{(-a_4)(b_4+a_4)(a_4+b_5)} \\
a_{23} &= a_9 + a_{12} \\
a_{26} &= a_{16} - a_{19} \\
a_{29} &= \frac{Gr}{(b_4-b_5)} \\
a_{32} &= \frac{Gmas(a_1+b_{10}L)}{(b_{10}+a_4)(b_{10}-b_9)} \\
a_{35} &= \frac{Gmas(a_1 \mp b_5L)}{(b_5+a_4)(b_5-b_4)} \\
a_{38} &= \frac{a_5(a_1-a_4L)}{(-a_4)} \\
b_3 &= a_1 - b \\
b_6 &= \alpha Sc \\
b_9 &= \frac{-b_7 + \sqrt{b_7^2 - 4b_6b_8}}{2b_6} \\
b &= M^2 + \frac{1}{k_1} \\
a_3 &= L - Sc \\
a_6 &= \frac{a_1 a_5}{a_4} \\
a_9 &= \frac{Gm}{b_9 b_{10}} \\
a_{12} &= \frac{Gmas a_5}{a_4 b_9 b_{10}} \\
a_{15} &= \frac{Gmas(a_1+b_{10}L)}{(b_{10})(b_{10}+a_4)(b_{10}-b_9)} \\
a_{18} &= \frac{Gr}{(b_5)(b_5-b_4)} \\
a_{21} &= \frac{Gmas(a_1+b_4L)}{(b_4)(b_4+a_4)(b_4-b_5)} \\
a_{24} &= a_{10} + a_{14} \\
a_{27} &= a_{17} - a_{21} \\
a_{30} &= \frac{Gmas(a_1-a_4L)}{(b_9+a_4)(a_4+b_{10})} \\
a_{33} &= \frac{Gmas(a_1-a_4L)}{(b_4+a_4)(a_4+b_5)} \\
a_{36} &= a_{29} - a_{34} \\
b_1 &= \alpha L \\
b_4 &= \frac{-b_2 + \sqrt{b_2^2 - 4b_1b_3}}{2b_1} \\
b_7 &= Sc + \alpha Kr.Sc - c \\
b_{10} &= \frac{-b_7 - \sqrt{b_7^2 - 4b_6b_8}}{2b_6} \\
a_1 &= \frac{-H}{1+R}, L = \frac{Pr}{1+R} \\
a_4 &= \frac{a_2}{a_3} \\
a_7 &= \frac{a_5(a_1-a_4L)}{a_4^2} \\
a_{10} &= \frac{Gm}{b_9(b_9-b_{10})} \\
a_{13} &= \frac{Gmas(a_1-a_4L)}{(-a_4)(b_9+a_4)(a_4+b_{10})} \\
a_{16} &= \frac{Gr}{b_4 b_5} \\
a_{19} &= \frac{Gmas a_5}{a_4 b_4 b_5} \\
a_{22} &= \frac{Gmas(a_1+b_5L)}{(b_5)(b_5+a_4)(b_5-b_4)} \\
a_{25} &= a_{11} + a_{15} \\
a_{28} &= a_{18} - a_{22} \\
a_{31} &= \frac{Gmas(a_1+b_9L)}{(b_9+a_4)(b_9-b_{10})} \\
a_{34} &= \frac{Gmas(a_1 \mp b_4L)}{(b_4+a_4)(b_4-b_5)} \\
a_{37} &= -a_{29} - a_{35} \\
b_2 &= L + \alpha a_1 - c \\
b_5 &= \frac{-b_2 - \sqrt{b_2^2 - 4b_1b_3}}{2b_1} \\
b_8 &= Kr.Sc - b
\end{aligned}$$

References

- [1] W. Tan, T. Masuoka, Stokes' first problem for a second grade fluid in a porous half-space with heated boundary, *Int. J. Non-Linear Mech.* 40 (2005) 515–522.
- [2] M.M. Rashidi, S.A. Majid, A. Mostafa, Application of homotopy analysis method to the unsteady squeezing flow of a second-grade fluid between circular plates, *Math. Probl. Eng.* 18 (2010) 706840.
- [3] T. Hayat, M. Qasim, S.A. Shehzad, A. Alsaedi, Unsteady stagnation point flow of second grade fluid with variable free stream, *Alexandria Eng. J.* 53 (2014) 455–461.
- [4] J. Hartmann, Hg-dynamics I theory of the laminar flow of an electrically conductive liquid in a homogenous magnetic field, *Det Kongelige Danske Videnskabernes Selskab Mathematisk-fysiske Meddelelser* 15 (1937) 1–27.
- [5] V.V.S. Murty, A. Gupta, N. Mandloi, A. Shukla, Evaluation of thermal performance of heat exchanger unit for parabolic solar cooker for off-place cooking, *Indian J. Pure Appl. Phys.* 45 (2007) 745–748.
- [6] N.K. Raja, M.S. Khalil, S.A. Masood, M. Shaheen, Design and manufacturing of parabolic trough solar collector system for a developing country Pakistan, *J. Am. Sci.* 7 (2011) 365–372.
- [7] R. Muthucumaraswamy, E. Geetha, Effects of parabolic motion on an isothermal vertical plate with constant mass flux, *Ain Shams Eng. J.* 5 (2014) 1317–1323.
- [8] N.S. Akbar, S. Nadeem, R.U. Haq, S. Ye, MHD stagnation point flow of Carreau fluid toward a permeable shrinking sheet: Dual solutions, *Ain Shams Eng. J.* 5 (2014) 1233–1239.
- [9] M. Sheikholeslami, D.D. Ganji, M. Gorji-Bandpy, Soheil Soleimani, Magnetic field effect on nanofluid flow and heat transfer using KKL model, *J. Taiwan Inst. Chem. Eng.* 45 (2014) 795–807.
- [10] M. Sheikholeslami, D.D. Ganji, M.M. Rashidi, Magnetic field effect on unsteady nanofluid flow and heat transfer using Buongiorno model, *J. Magn. Magn. Mater.* 416 (2016) 164–173.
- [11] M. Sheikholeslami, M. Gorji-Bandpy, D.D. Ganji, MHD free convection in an eccentric semi-annulus filled with nanofluid, *J. Taiwan Inst. Chem. Eng.* 45 (2014) 1204–1216.
- [12] M. Sheikholeslami, R. Ellahi, Three dimensional mesoscopic simulation of magnetic field effect on natural convection of nanofluid, *Int. J. Heat Mass Transf.* 89 (2015) 799–808.
- [13] M. Sheikholeslami, K. Vajravelu, M.M. Rashidi, Forced convection heat transfer in a semi annulus under the influence of a variable magnetic field, *Int. J. Heat Mass Transf.* 92 (2016) 339–348.
- [14] M. Sheikholeslami, A.J. Chamkha, Electrohydrodynamic free convection heat transfer of a nanofluid in a semi-annulus enclosure with a sinusoidal wall, *Numer. Heat Transfer, Part A* 69 (2016) 781–793.
- [15] M. Sheikholeslami, A.J. Chamkha, Flow and convective heat transfer of a ferro-nanofluid in a double-sided lid-driven cavity with a wavy wall in the presence of a variable magnetic field, *Numer. Heat Transfer, Part A* 69 (2016) 1186–1200.
- [16] M. Sheikholeslami, Effect of spatially variable magnetic field on ferrofluid flow and heat transfer considering constant heat flux boundary condition, *Eur. Phys. J. Plus* (2014) 129–248.
- [17] H.R. Kataria, H.R. Patel, Rajiv Singh, Effect of magnetic field on unsteady natural convective flow of a micropolar fluid between two vertical walls, *Ain Shams Eng. J.* (2015), <http://dx.doi.org/10.1016/j.asej.2015.08.013>.
- [18] M. Sheikholeslami, D.D. Ganji, M.Y. Javed, R. Ellahi, Effect of thermal radiation parameter on magnetohydrodynamics nanofluid flow and heat transfer by means of two phase model, *J. Magn. Magn. Mater.* 374 (2015) 36–43.
- [19] M. Sheikholeslami, T. Hayat, A. Alsaedi, MHD free convection of Al_2O_3 -water nanofluid considering thermal radiation parameter: a numerical study, *Int. J. Heat Mass Transf.* 96 (2016) 513–524.
- [20] H.R. Kataria, A.S. Mittal, Mathematical model for velocity and temperature of gravity-driven convective optically thick nanofluid flow past an oscillating vertical plate in presence of

- magnetic field and radiation, *J. Nigerian Math. Soc.* 34 (2015) 303–317.
- [21] S. Nadeem, R.U. Haq, N.S. Akbar, Z.H. Khan, MHD three-dimensional Casson fluid flow past a porous linearly stretching sheet, *Alexandria Eng. J.* 52 (2013) 577–582.
- [22] H.R. Kataria, A.S. Mittal, Velocity, mass and temperature analysis of gravity-driven convection nanofluid flow past an oscillating vertical plate in presence of magnetic field in a porous medium, *Appl. Therm. Eng.* 110 (2017) 864–874.
- [23] F. Abbasi, S. Shehzad, T. Hayat, B. Ahmad, Doubly stratified mixed convection flow of Maxwell nanofluid with heat generation/absorption, *J. Magn. Magn. Mater.* 404 (2016) 159–165.
- [24] S. Shehzad, T. Hayat, A. Alsaedi, Three-dimensional MHD flow of casson fluid in porous medium with heat generation, *J. Appl. Fluid Mech.* 9 (2016) 215–223.
- [25] Constantin Fetecau, Dumitru Vieru, Corina Fetecau, Ioan Pop, Slip effects on the unsteady radiative MHD free convection flow over a moving plate with mass diffusion and heat source, *Eur. Phys. J. Plus* 130 (2015) 6.
- [26] H.R. Kataria, H.R. Patel, Radiation and chemical reaction effects on MHD Casson fluid flow past an oscillating vertical plate embedded in porous medium, *Alexandria Eng. J.* 55 (2016) 583–595.
- [27] S. Sengupta, N. Ahmed, Chemical reaction interaction on unsteady MHD free convective radiative flow past an oscillating plate embedded in porous media with thermal diffusion, *Adv. Appl. Sci. Res.* 6 (2015) 87–104.
- [28] H.R. Kataria, H.R. Patel, Soret and heat generation effects on MHD casson fluid flow past an oscillating vertical plate embedded through porous medium, *Alexandria Eng. J.* 55 (2016) 2125–2137.
- [29] A. Khan, I. Khan, F. Ali, S. Shafie, Effects of wall shear stress MHD conjugate flow over an inclined plate in a porous medium with ramped wall temperature, *Math. Probl. Eng.* (2014), <http://dx.doi.org/10.1155/2014/861708>.
- [30] A. Khalid, I. Khan, S. Shafie, Exact solutions for free convection flow of Nano fluids with ramped wall temperature, *Eur. Phys. J. Plus* 130 (2015) 57.
- [31] G.S. Seth, A.K. Singha, R. Sharma, MHD natural convection flow with hall effects, radiation and Heat absorption over an exponentially accelerated vertical Plate with ramped temperature, *Ind. J. Sci. Res. Technol.* 5 (2015) 10–22.
- [32] G.S. Seth, S.M. Hussain, S. Sarkar, Hydromagnetic natural convection flow with heat And mass transfer of a chemically reacting and heat Absorbing fluid past an accelerated moving vertical plate with ramped temperature and ramped surface Concentration through a porous medium, *J. Egypt. Math. Soc.* 23 (2015) 197–207.
- [33] T. Hayat, M. Nawaz, M. Sajid, S. Asghar, The effect of thermal radiation parameter on the flow of a second grade fluid, *Comput. Math. Appl.* 58 (2009) 369–379.
- [34] S. Samiulhaq, D. Ahmad, I. Vieru, S. Khan Shafie, Unsteady magnetohydrodynamic free convection flow of a second grade fluid in a porous medium with ramped wall temperature, *PLoS ONE* 9 (5) (2014) e88766, <http://dx.doi.org/10.1371/journal.pone.0088766>.
- [35] K. Das, R.P. Sharma, A. Sarkar, Heat and mass transfer of a second grade MHD fluid over a convectively heated stretching sheet, *J. Comput. Des. Eng.* (2016), <http://dx.doi.org/10.1016/j.jcde.2016.06.001>.
- [36] S. Rosseland, *Astrophysik und atom-theoretische Grundlagen*, Springer-Verlag, Berlin, 1931.